Computation Modeling of Reinforced concrete beams using Fictitious crack model

FINAL YEAR PROJECT UG 2016

By

MUHAMMAD JAHANGIR
TALHA NAVEED
AHMAD REHAN KASHIF

NUST Institute of Civil Engineering
School of Civil and Environmental Engineering
National University of Sciences and Technology, Islamabad, Pakistan

2020

This is to certify that the

Final Year Project Titled

"Computation Modeling of Reinforced concrete beams using Fictitious crack model"

Submitted by

MUHAMMAD JAHANGIR
TALHA NAVEED
AHMAD REHAN KASHIF

has been accepted towards the requirements

for the undergraduate degree

in

CIVIL ENGINEERING

____

Dr. Muhammad Usman Hanif
Structural Engineering Department
NUST Institute of Civil Engineering
School of Civil and Environmental Engineering
National University of Sciences and Technology, Islamabad, Pakistan

ACKNOWLEDGEMENTS

In the name of God, the most merciful, the most beneficent, all glory to Him, the creator of the heavens and divine Prophet Muhammad (S.A.W), his last prophet.

We are, first, indebted to Almighty God, without Whose grace and protection, we should have never done what we have ended up eventually accomplishing.

We would like to convey our gratitude to our beloved parents and teachers for their endless love and guidance throughout our lives, and for making us realize our dreams.

Our Civil Engineering Bachelor 's journey, especially our thesis year, has been a remarkable experience for us all and we can't be more grateful to all people who have been part of this journey with us.

We are at a loss of words to convey the appreciation to all the people who inspired, supported, guided us and enabled us to complete this journey successfully.

We would like to begin by expressing our gratitude to our supervisor Dr Muhammad Usman Hanif for his consistent mentoring during this trip. During this pursuit he remained a source of unique and useful guidance for us for over a year.

His unprecedented experience in concrete construction has also opened our eyes to this specific field of engineering practice, which we were unfamiliar to at first. He's always motivated us to stay focused on achieving our goals. His experience was instrumental in helping us demarcate the course of our work and develop the study in detail. His inexorable encouragement supported us tremendously through our time of study and development as well as in improving our expertise in science literature. Our deepest and sincere gratitude to him for making us become hard working, professional and a better individual.

Dedication

To

Our Advisor Dr. Muhammad Usman Hanif

&

Our Families and Friends

TABLE OF CONTENTS

LIST OF FIGURES

Chapter 1

Chapter 2

Chapter 3

Chapter 4

LIST OF TABLES

NOTATIONS AND SYMBOLS

FPZ	Fracture process zone
FCM	Fictitious crack model
LEFM	Linear Elastic Fracture Mechanics
CZM	Cohesive zone model
SHM	Structural Health monitoring
SLF	Structural Local Frequency
SGF	Structural Global Frequency
SM	Stiffness Matrix
CMM	Consistent Mass Matrix
DM	Damping Matrix
MFA	Modal Frequency Analysis
DAM	Dynamic Analysis Method
CCM	Concrete cracks modeling
SAM	Static Analysis Method
PM	Prism Modeling
TCM	Tension Crack Modeling
fc’	28-day compressive strength of concrete
Fy	Tensile strength of steel
Ec	Modulus of elasticity of concrete.

Es	Modulus of elasticity of steel
Hc	Crack width
Wc	Critical crack width
G1 and G2	Residual stresses and moment at the intersection
A	Modification factor
Φ	Relative rotation
Z	Damping ratio
Nc	Concrete elongation
Nct	Concrete elongation at ultimate tensile strength
K	Element stiffness matrix
Kmod	Modified stiffness matrix
F(t)	Excitation force
G	Function defines undamaged parts and cracked regions
~~Fcu~~fcu	Ultimate compressive strength
~~Fct~~fct	Concrete tensile strength

CHAPTER 1

INTRODUCTION

1.1 General

Concrete is the widely available construction material in the world, and fairly inexpensive as it has a broad variety of qualities, such as, it can be molded to any shape, high compressive strength and also it provides resistance to vibration. But since it is mostly porous and weak in tensile strength, it is prone to the formation of micro-cracks that could induce low strength. However, concrete is strong in compression which makes it a versatile material. When combined with another material (steel) which is strong in tension, we can take the best out of concrete in terms of strength and stability. Concrete, with the introduction of structural material like steel, then can be used in beams, columns, slabs, etc. It is perceived as a success boost and a material that is delicate. That is because there is difference in the behavior of concrete failure mechanism. Concrete is considered a virtually breakable material in modern fracture mechanics (Anderson, 2017).

Concrete is usually combined with a material strong in tension to enhance its strength properties. But with the enhancement of properties, the understanding of behavior becomes complicated. Concrete is considered as ceramic material (glass, rock and concrete are ceramic materials), and its material behavior is not completely understood, even after a century of research. There are various concrete models proposed in the past which attempt to explain the material behavior of concrete like, elastic models, elasto-plastic models, fracture models, micro plane and continuum models, to name a few.

Commonly used concrete models ignore the tensile behavior of concrete as they consider a linear elastic behavior of concrete and the onset of maximum tensile strength is ignored. However, displacement-controlled tests show that concrete show softening behavior in post-peak tensile stress-strain response. This softening behavior of concrete is non-linear in nature, and has been described in detail by Fictitious Crack Model(FCM).

1.2 Fictitious Crack Model

Arne Hillerborg proposed the fictitious crack model in 1976 (Hillerborg et al., 1976). Hillerborg divided the stress-strain deformation process in the following zones:

1: Linear elastic zone

2: Fictitious crack or fracture process zone (FPZ) (Sima et al., 2008)

3: Actual crack formation zone (the onset of critical crack width)

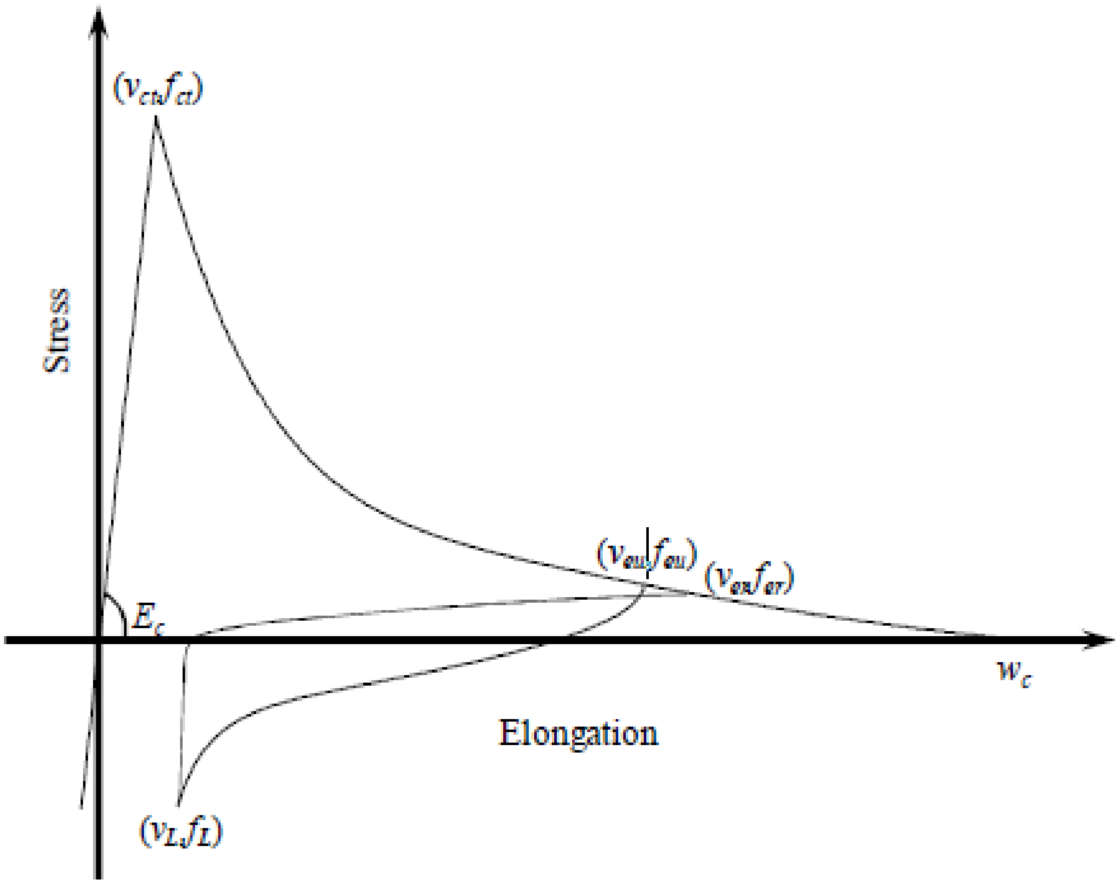

Figure 1. 1 (Fictitious crack model crack zones)

1.2.1 Linear elastic zone:

This is the zone in which the stress and strain are directly proportional to each other till the maximum tensile strength reached.

1.2.2 Fictitious crack zone:

It exists before the true crack zone, in this region cracks are cohesive and able to heal themselves when unloaded and have stress values. In this region at the tip of the crack we had peak stress equal to the tensile strength (Bazant & Planas., 1998).

1.2.3 Actual crack formation zone:

This region starts after the fictitious crack zone when critical crack width reached in this zone the cracks are visible and of no stress value this is the onset of critical crack width.

1.2.4 Assumptions of fictitious Crack model:

1. Concrete acts in linear elastic manner before reaching the ultimate tensile strength.

2. Tension is not expected to decrease to zero at the onset of crack.

3. Once the crack width exceeded the critical crack width, crack is formed.

The idea of this research is to utilize the fictitious crack model, that describes the crack formation and crack propagation, in computational modeling of concrete failure mechanism. The realistic description of behavior can be useful tool in development of better structural health monitoring practices.

1.3 Structural Health Monitoring (SHM)

Structural health monitoring (SHM) is applied to structures applying a hazard prevention and classification technique. Damage is defined as such changes of material and/or geometric properties to a structural framework including boundary conditions that affect the performance of the structure adversely. The SHM process involves long-lasting surveillance of the structures by means of regular measurements of frequency responses from a range of sensors, identification, and comparative analysis to measure the current damage for the safety of the structure. The outcomes from this process are regularly tracked by SHM. SHM is used for identifying damages following major events, such as earthquakes or fires, to provide precise information about damage.

Structural Health monitoring has excelled significantly in various fields like automotive and aerospace. In civil engineering structures, especially RC structures, there has not been a significant development in SHM paradigm due to:

1. Massiveness of structure, lack of reproducibility in the lab.
2. Complex behavior of the constituent materials
3. Complex failure mechanism of concrete.
4. Every structure is unique – generalization is a challenging task.
5. The fracture behavior of concrete is not completely understood and is totally ignored in the analysis of the structures (tensile strength of concrete).

One major reason in applying SHM to civil infrastructure is that every structure is unique and massive, so lab testing is not possible. A peculiar characteristic of SHM is that it needs to remain tailored around the long-term assessment of structural efficiency and safety. So, there is a need of SHM for damage detection. The approaches of SHM are vibration based and wavelet based (Rytter, 1993).

1.3.1 Why Structural health monitoring?

Structural health monitoring is important because it addresses the key issues that a structure goes through when damaged. These are given below:

1. Report the presence of structural damage

2. The damage is located

3. The extent of the strength loss is assessed

Civil Engineering structure are often huge, complicated, and damage-insensitive and therefore the precise estimate of certain structural parameters involves significant amount of detailed knowledge. Commonly used SHM approach is reduction of natural frequencies using modal analysis.

1.4 Problem Statement

The reduction in natural frequency-based method incorporate certain simplifications for the purpose of making the model efficient which does not reflect the nonlinear behavior. Concrete exhibits a highly nonlinear behavior and after the formation of crack, nonlinear behavior can be characterized and used in damage assessment. LEFM ignores the nonlinearities related to concrete fracture and does not correctly quantify tensile strength at the crack edge. We ought to figure out a little more about tension near crack tip.

LEFM is unable to react to several executables. Types include:

1. LEFM does not recognize the principle of fracture energy
2. Cannot describe fictitious crack zone.

It is obvious that there must be some cohesive zone between the cracked region and the uncracked region. The fracture process zone (FPZ) has been defined for such a region. FPZ comprises several microscopic cohesive cracks situated closer to the crack edge. As a crack expands, those micro cracks unite which form a cohesive framework that causes an original crack to form later. The FPZ serves as a bridging field between the zone that has been cracked and that which has not been cracked.

Fracture mechanics should seek to answer the following questions in explanatory manner:

1. What really is the maximum acceptable crack width allowed under service loading?
2. How long will a crack take to rise to the highest allowable crack size from a certain initial size?
3. If a certain prior damage occurs, then what is the reliability of the structure?
4. How the structure be inspected for cracks?

Such concerns were not resolved long until around the Hillerborg model (Sundara Raja Iyengar et al., 2002). It shows tensile behavior plays important role in static and dynamic analysis. There is also a need for SHM technique that depends on only a few strength indices to model the complete structure. Researchers are always interested in the convenience of developing the complete material behavior based on the fewer strength indices taken from the laboratory testing as possible.

The above reasons for the lack of SHM in RC structures based on cohesive process zone are reflected in the objectives.

1.5 Objectives

Considering the components detailed out in the problem statement, the objectives of our thesis are enlisted as follows:

1. To study the tensile behavior of concrete using Fictitious crack model.

2. To model a reinforced concrete beam under four-point bending and find its load-deflection while predicting crack propagation.

3. To carry out dynamic analysis to evaluate natural frequencies and find the reduction in natural frequencies with increasing damage.

1.6 Scope

1. The scope of this research is limited to reinforced beams only.

2. The experimental results for comparison will be taken from the reference research (Hamad et al., 2011, 2013).

CHAPTER 2

LITERATURE REVIEW

Throughout most of the history, major attempts have been made towards building predictive simulations to forecast concrete fracturing action. The computational process based on the finite-element method was typically categorized into two approaches: a smeared crack approach and a discrete crack approach in the field of fracture mechanics.

The crack is typically modeled on a finite element grid, and its distribution is measured through increasing the material's stiffness and strength. Many models consider concrete as almost a breakable substance with no cohesive behavior throughout tensile region. (Hamad et al., 2013)

Hillerborg et al., established the Cohesive Zone Model (CZM) (Hillerborg et al., 1976), that further presumes how stresses impact the crack opening width. FCM is really the strongest basic mechanics model for fracturing although it offers simple and clear calculations for just a rational estimate of crack propagation throughout concrete. The FCM can be used for studying fracture processes throughout concrete under monotonous as well as cyclic loadings. The model mainly applies to mode I fractures.

2.1 Concept of fracture energy

Fracture energy is defined as the energy needed to grow crack surface area. It is indeed a substance property that is not structure dependent. The concept is that, even a unit area becomes specified and that the effect for whole scale should be excluded. The fracture energy may also be defined as that of the sum of energy generated by surface and energy separating the surface. Fracture energy is indeed a driving function. Fracture strength is also of the utmost significance throughout the determination of maximum tensile strength.

It is expressed as:

Area under the curve of the onset of the softening curve of stress strain relationship of concrete in tension.

2.2 Concept of characteristic length

Hillerborg (Hillerborg et al., 1976) also expressed an important parameter which he renamed as Hillerborg characteristic length (L) which calculated as follows,

$L = [(E*G)/\sigma\hat{}\ (2)]$

Where

σ = critical stress value

G = fracture energy

L= characteristic length

E= Young's Modulus

2.3 Concept of fictitious crack zone

The peak is equivalent to the maximum tensile strength at the crack tip (Bažant, 2004). FPZ crack spreads when the critical stress is equal to a concrete's tensile strength. FPZ comprises several microscopic cohesive cracks situated closer to the crack edge. As a crack expands, those micro cracks unite which form a cohesive framework that causes an original crack to form later. The FPZ serves as a bridging field between the zone that has been cracked and that which has not been cracked.

2.4 Concept of crack modeling:

With the review of literature (Hamad et al., 2013, 2015) we were able to grasp the concept of modeling of concrete cracking. Throughout the last thirty years, extensive work has been conducted into the process of concrete crack formation. A broad variety of modeling methods, including plasticity model, micro plane models and fracture mechanics, have been established in terms of computational models for concrete. Models based on a mechanical fracture approach were considered suitable for simple calculations of the fracturing process.

The FCM has been one of the types for fracture mechanics ideal for the analysis of concrete cracking. It often defines cracks which uses cohesive force.

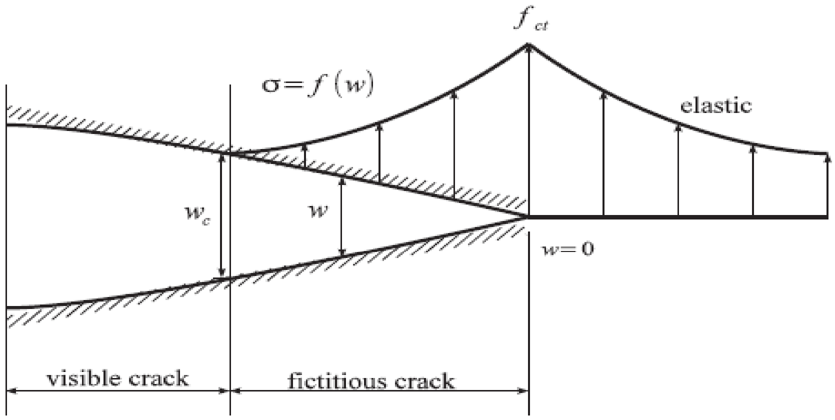

Cohesive stress distribution ahead of a visible crack. The symbols are defined in the text and the nomenclature.

Figure 2. 1 (Cohesive stress distribution ahead of visible crack)

Such compact stresses, which arise in the fracture phase zone (FPZ), are attributable through stress transfer amongst micro-cracks plus certain tension which is mostly in friction due to aggregates and materials of homogeneous faces. In the Research paper, (Hamad et al., 2013) researchers were using the FCM to build a single crack mid-span model of both the single bending cracking action of a plain concrete (PC) prism.

These same constitutional laws were introduced in their process to investigate cyclical bending, since the tensile strength of the concrete (fct) was believed and then this concept was implemented. However, that impact of the crack has been intended to extend over a region of crack width (hc), considered an elastic zone. This same width of such an area is also an essential parameter of the model because of rigidity of the cracked area which is defined. This crack width had been considered as being half the total cross-sectional height and the authors also confirmed that perhaps a good agreement to experimental measurements has been obtained in setting hc to half this same height of the cross-section. The substance on the direction of creation of the crack was believed to be in one of three plausible states:

1. Before crack formation in linear elastic state
2. A fracturing condition in which substance is weakened by the cohesive power of the FPZ

3. That zero-stress condition where even the width of that same crack is smaller than critical width (wc).

That bending action among RC beams with four-point bending test may as well be modeled with the same principle using a combination of monotonic and cyclic flexural actions of the PC prism form. Unlike other PC prisms, several cracks exist within rapidly filled RC beams. Tension cracks generally occur whenever bending tension at a certain part of the beam exceeds maximum tensile strength of the concrete. The cracked RC beam layout may well be separated into variety of regions such as cracked and uncracked. The location where the cracks develop when the concrete tensile force exceeded needs advanced information. Past studies on RC beams have already shown that cracks seem to be approximately proportional to the difference between shearing connections and spacing (Hamad et al., 2013).

2.5 Main Findings of the research:

Some of the finding of the research are as follows:

- Current concrete models make design conservative, but modeling is getting complicated.
- Current design practices consider concrete elastic and ignores the tensile behavior of concrete.
- Recent research shown that the FE software-based methods are not adequate for accurate damage assessment of the structures.
- The fracture behavior of concrete is very complex so there is a need to study it as accurately as possible
- Tensile behavior plays important role in static and dynamic analysis
- There is a need for SHM technique that depends on only a few strength indices to model the complete structure.

CHAPTER 3

RESEARCH METHODOLOGY

The research is divided into three parts:

3.1 Study of crack in prism:

To study a single crack in a beam the following arrangement is used:

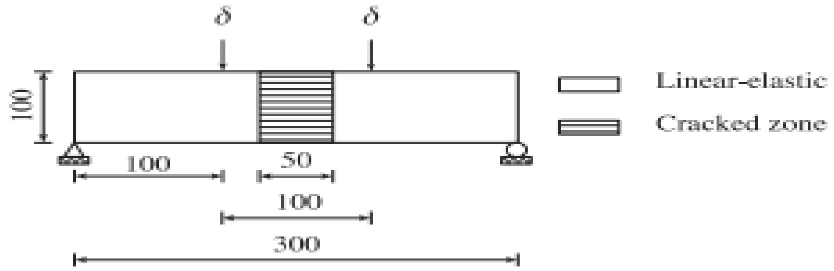

We have to perform the monotonic and cyclic four-point bending tests on standard 300 mm * 100 mm * 100 mm PC on displacement-controlled machine but due to pandemic we were unable to perform tests.

The actual procedure for the casting is as follows:
A single concrete mix, with a maximum aggregate size of 10 mm and ordinary Portland cement grade 36.27, was used for all prisms for the experiments.

The mechanical properties of material are as follows:

Table 3. 1 (Mechanical properties of concrete material) (Hamad et al., 2013)

Prism name	Fcr (Mpa)	σFcr (Mpa)	Ec (Gpa)	σEc (Gpa)
PIII-CT PIII-MT	36.27	0.29	31.59	0.16

P: prism; MT: monotonic test; CT: cyclic test.

The weight proportions of concrete mixes are as follows:

Table 3. 2 (Weight proportions of concrete mixes) (Hamad et al., 2013)

Material	Density (Kg/m^3)
Coarse aggregate	1025
Fine aggregate	835
Cement	320
Water	181

The prisms were cast on two weeks. In total, 11 prisms were casted but we were not able to perform the test therefore we the experimental results of Hamad and Owen research paper (Hamad et al., 2011, 2013, 2015)

From the previous researches, it is known that the cracked region thickness, hc, is equal to the half of the depth of the beam (Hamad et al., 2013)
Now to study the crack at a certain displacement, first of all the compatibility at the both ends of the prism should be ensured. This is done using the following equations by (Ulfkjrer et al., 1995)(Sundara Raja Iyengar et al., 2002)

$$G1 = \theta 1 + \frac{\left(M - Ws\frac{(L1 + L2)^2}{2}\right)}{3EcIc}L1 + \frac{(M - Ws\frac{(L1 + L2)^2}{2}}{EcIc}L2 + \frac{Ws}{EcIc}\left(\frac{(L1 + L2)^3}{3} - \frac{L1^3}{8} - \frac{L1^2L2}{6}\right) - \frac{\delta}{L1}$$

$$G2 = M - Kcr\theta 1$$

Where Kcr is proposed by (Ulfkjrer et al., 1995) given as:

$$Kcr = \frac{Mc}{\theta 1}$$

Here G1 and G2 are the residual stresses and moment at the intersection which must be equal to the zero to satisfy the compatibility. To obtain compatibility, Newton-Raphson iterative solver is used so that both G1 and G2 becomes zero.

$$\begin{bmatrix} \theta 1 \\ M \end{bmatrix} = \begin{bmatrix} \theta 1i \\ Mi \end{bmatrix} - J^{-1} \begin{bmatrix} G1 \\ G2 \end{bmatrix}$$

Here Jacobian Matrix is found by (Ulfkjrer et al., 1995)(Sundara Raja Iyengar et al., 2002) as follows:

$$\begin{bmatrix} 1 & \dfrac{L1}{3EcIc} \\ -\dfrac{\partial M}{\partial \theta} & 1 \end{bmatrix}$$

Here as a starting value M and Theta1 are taken as zero and kcr is calculated from the geometric properties of the prism which is proposed by (Ulfkjrer et al., 1995)(Sundara Raja Iyengar et al., 2002) as:

$$Kcr = \frac{2EcIc}{Hc}$$

and then G1 is calculated. Now for the G2 we will perform the cross-sectional analysis on the prism which is continued as follows by (Ulfkjrer et al., 1995):

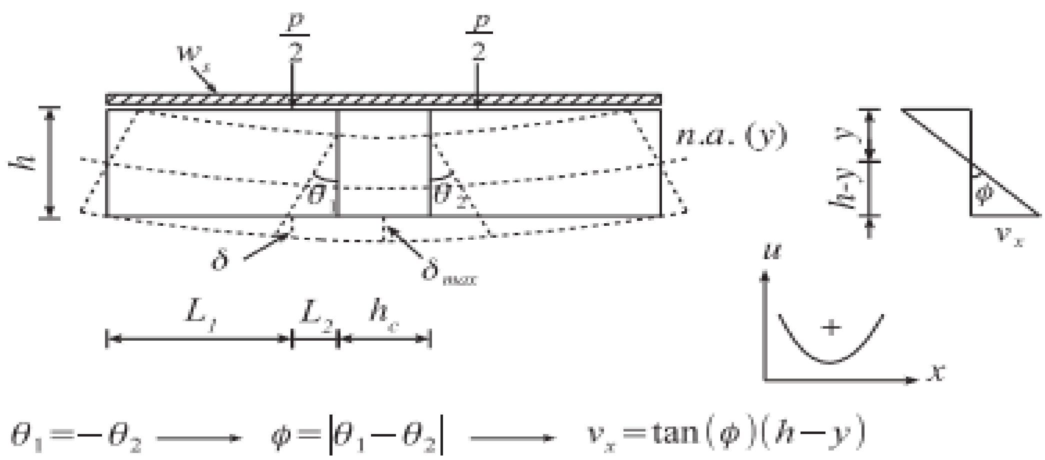

From the value of Theta1, Phi is calculated. Then the neutral axis is assumed and Vx is calculated as proposed by (Sundara Raja Iyengar et al., 2002) :

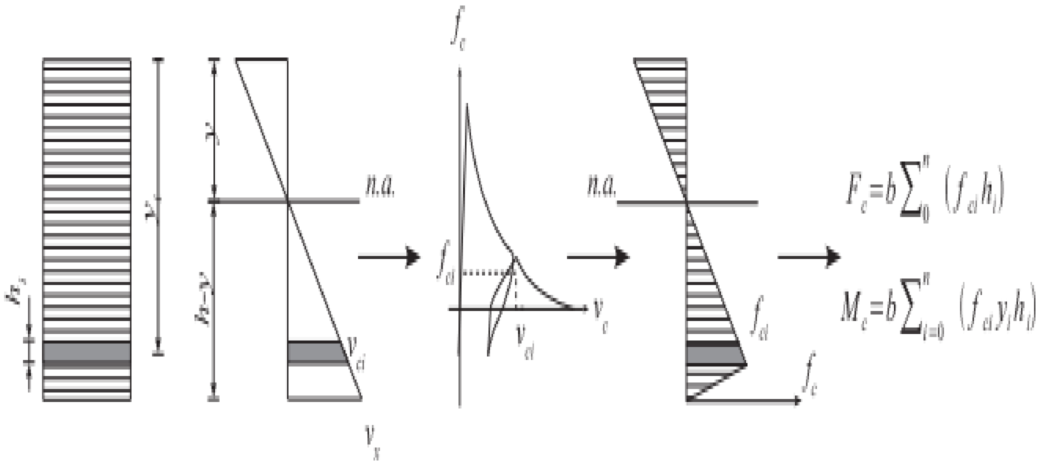

From the value of Vx and Phi, elongation profile is developed.
Now this elongation profile is converted into the stress profile using the following methods:

3.2 For the Tension Region:

For the tension region, fictitious crack model is used. Fictitious cracks are incorporated in our model as they play a vital role in the crack formation. Following are the equations given for the fictitious crack model.
According to (Hans W. Reinhardt et al., 1986) we have this equation:

$$Fc = Fct\ [\{1 + (C1(W/Wc)^3\}\exp\left[-\mathrm{C2}\left(\frac{W}{Wc}\right)\right] - \left(\frac{W}{Wc}\right)(1 + C1^3)\exp(-C2)]$$

Where Vc is proposed by (Hans W. Reinhardt et al., 1986) as follows

$$Vc = \frac{fct * hc}{Ec} + w$$

And according to (Hordijk, 1992) we have this equation

$$Wc = 5.14\ \frac{Gf}{Fct}$$

And by (Phillips & Binsheng, 1993) we have this equation

$$Gf = 43.3 + 1.13fcu$$

And the constants C1 and C2 are 3 and 6.93, respectively.

Using these equations, the stress elongation profile is developed for the tension region of the beam.

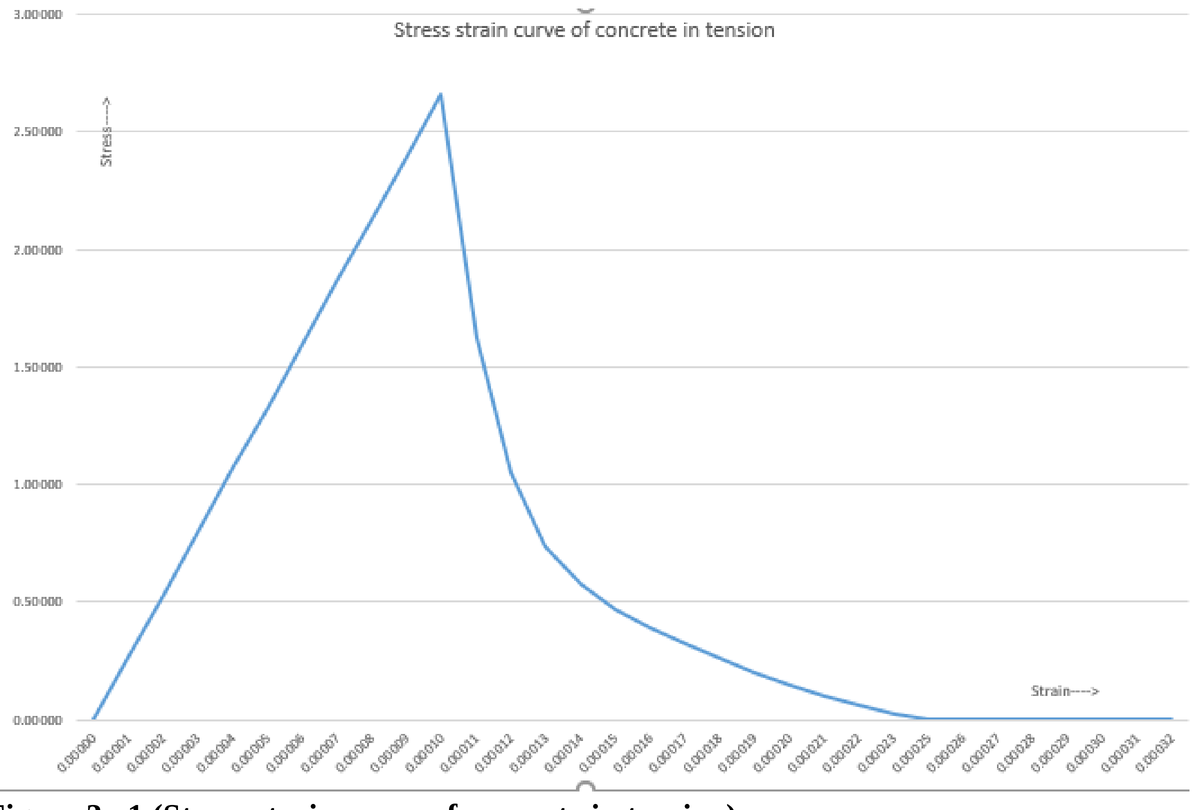

Figure 3. 1 (Stress strain curve of concrete in tension)

3.3 For Compression region:

For the compression region, Carriera and Chu paper is used.

Following are the equations used by (H. W. Reinhardt, 1984) .

$$\varepsilon o \ = (7.1\, fc' + 1680)10^{-6}$$

And

$$fc' = \frac{fc'\, \beta(\ \varepsilon/\varepsilon o\ )}{[\ \beta - 1 + (\frac{\varepsilon}{\varepsilon o})^{\wedge\beta}\ ]}$$

$$\beta = \frac{1}{[1 - \left(\frac{fc'}{Eo\varepsilon o}\right)]}$$

Where:

- fc'= Maximum stress
- β = Material parameter
- ε = Concrete Stain
- εo = Corresponding strain at maximum stress
- Eo = Initial Tangent Modulus

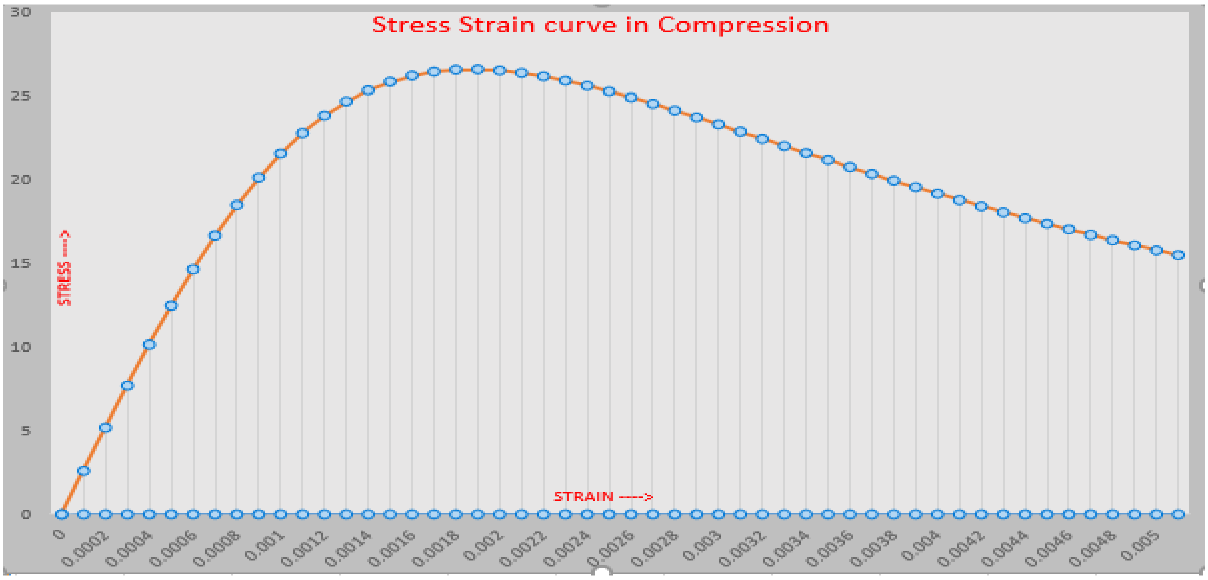

Figure 3. 2 (Stress strain curve of concrete in compression)

Now using both equations for tension and compression region, the cross-section of the beam is divided into the strips and for each strip stress is calculated and plotted. From this plot, stresses are converted into forces and checked if the forces become zero. If it became zero, then the values of Mc are used otherwise neutral axis is checked and the whole process it again performed until the Forces becomes zero.

This Mc is used to calculate Kcr as follows which was proposed by (Ulfkjrer et al., 1995):

$$Kcr = \frac{Mc}{\theta 1}$$

And then G2 is calculated. If G1 and G2 is zero, then the compatibility is ensured and Moment and Rotation for the specific displacement is finalized. Otherwise the new moment and theta1 are found and the whole process is iterated until G1 and G2 becomes zero.

Following is the flowchart for our process:

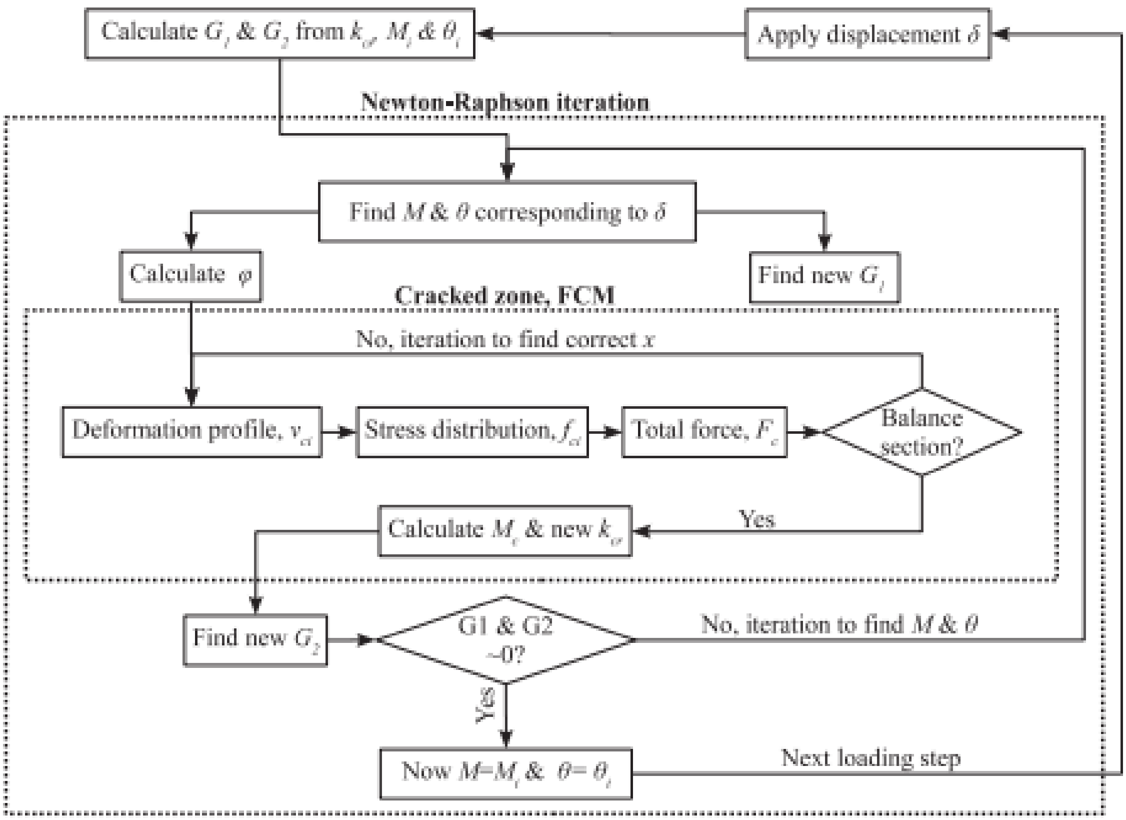

Figure 3. 3 (Flowchart for finalized moment and rotation) (Hamad et al., 2013)

Then this finalized moment is used to calculate the deflection proposed by (Ulfkjrer et al., 1995) as follows:

$$\delta max = \delta\left(1+\frac{L2}{L1}\right)-\frac{\left(M-Ws\frac{(L1+L2)^{1}}{2}\right)}{3EcIc}L1L2-\frac{\left(M-Ws\frac{(L1+L2)^{1}}{2}\right.}{2EcIc}L2^{2}$$
$$-\frac{Ws(L1+L2)}{EcIc}\left(\frac{(L1+L2)^{3}}{8}-\frac{L1^{3}}{8}-\frac{L1^{2}L2}{8}\right)+\frac{Hc\theta 1}{4}$$

And the load is calculated from the moment.
The load and deflection are calculated for each displacement and plotted.

3.4 For the single crack:

Following are the arrangements used for the single crack in a beam.

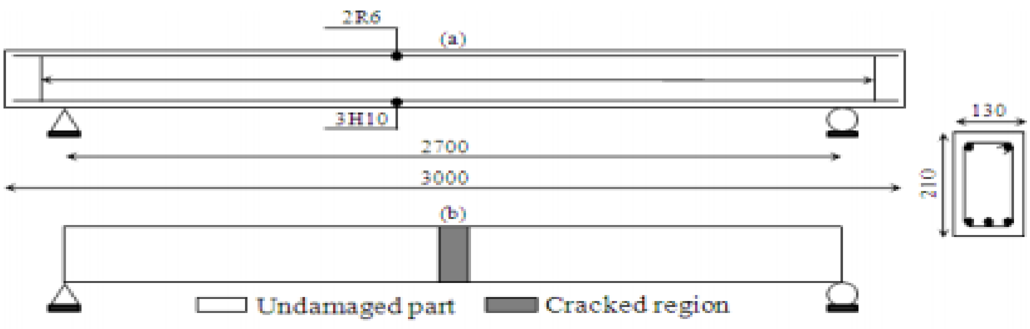

Now the beam is divided into three parts.
Two parts are undamaged, and one part is damaged.
The damaged part is modelled same as the prism.
Following are the mechanical properties used for the study of a single crack in a beam

Table 3. 3 (Mechanical properties of RC concrete used for the study of a single crack in a beam) (Hamad et al., 2013)

Material	**Compressive strength (N/mm^2)**	**Tensile strength (N/mm^2)**	**Modulus of elasticity (KN/mm^2)**
Concrete	30	3	30
Steel	-	250,400	200

Now to study the different damage levels, we need to study the rotational stiffness of the beam that is changing with each damage level.
For that we need moment and rotation.
The same method as used for the analysis of prism is used and using Newton-Rapson iterative solver, the moment and Rotation are calculated and plotted.

3.5 For dynamic Analysis:

For the dynamic analysis, we used the following equation to plot the response of the beam.

$$[M]\ddot{U} + [C]\dot{U} + [K]U = F(t)$$

Here we need three matrices which are global mass, damping and stiffness matrices.

$$M = \frac{\bar{m}l}{420}\begin{bmatrix} 156 & 22l & 54 & -13l \\ 22l & 4l^2 & 13l & -3l^2 \\ 54 & 13l & 156 & -22l \\ -13l & -3l^2 & -22l & 4l^2 \end{bmatrix}$$

Consistent mass matrix is used for the computation instead of lumped mass matrix as it gives more accurate results (Hamad et al., 2013) .
Following the matrix used to calculate the mass matrix.
The stiffness matrix is of two types:

1. Damaged
2. Undamaged parts

3.5.1 For undamaged part:

$$K = \begin{bmatrix} \frac{12EcIc}{l^3} & \frac{6EcIc}{l^2} & -\frac{12EcIc}{l^3} & \frac{6EcIc}{l^2} \\ \frac{6EcIc}{l^2} & \frac{4EcIc}{l} & -\frac{6EcIc}{l^2} & \frac{2EcIc}{l} \\ -\frac{12EcIc}{l^3} & -\frac{6EcIc}{l^2} & \frac{12EcIc}{l^3} & -\frac{6EcIc}{l^2} \\ \frac{6EcIc}{l^2} & \frac{6EcIc}{l} & -\frac{6EcIc}{l^2} & \frac{4EcIc}{l} \end{bmatrix}$$

3.5.2 For damaged part:

$$\boldsymbol{K}mod = \begin{bmatrix} \frac{12EcIc}{Hc^3} & \frac{6EcIc}{Hc^2} & -\frac{12EcIc}{Hc^3} & \frac{6EcIc}{Hc^2} \\ \frac{6EcIc}{Hc^2} & \frac{3EcIc}{Hc}+\frac{\alpha}{2} & -\frac{6EcIc}{Hc^2} & \frac{3EcIc}{Hc}-\frac{\alpha}{2} \\ -\frac{12EcIc}{Hc^3} & -\frac{6EcIc}{Hc^2} & \frac{12EcIc}{Hc^3} & -\frac{6EcIc}{Hc^2} \\ \frac{6EcIc}{Hc^2} & \frac{3EcIc}{Hc}-\frac{\alpha}{2} & -\frac{6EcIc}{Hc^2} & \frac{3EcIc}{Hc}+\frac{\alpha}{2} \end{bmatrix}$$

Where α is the modification factor corresponding to the end rotation and moment calculated from FCM model.

The damping matrix proposed by (Clough & Penzien, 2010) is as followed:

$$Cg = aoMg + a1Kg$$

Where,

$$\begin{Bmatrix} ao \\ a1 \end{Bmatrix} = \frac{2\zeta}{\omega m + \omega n} \begin{Bmatrix} \omega m \ \omega n \\ 1 \end{Bmatrix}$$

Now ζ is taken as 5% damping and ωm and ωn are taken as the 1st and 4th undamped natural frequency of the system (Clough & Penzien, 2010) .
From these matrices, global matrices are formed, and dynamic analysis is performed. Sine sweep wave is applied to the beam at a distance of 1.275 m from the left support and displacement response is noted at this distance. Then this response is converted into the RMS value and plotted, and the peak obtained is the resonant frequency of the system. The frequency range set was 31 to 57Hz and stepped approach is used with a step size of 0.04Hz.

CHAPTER 4

ANALYTICAL MODELING RESULTS

4.1 Results for the prism modelling:

First part of the research was to study the crack in a prism. As a result, we developed a model to study its behavior and developed a load displacement curve for the prism.

Following are the results:

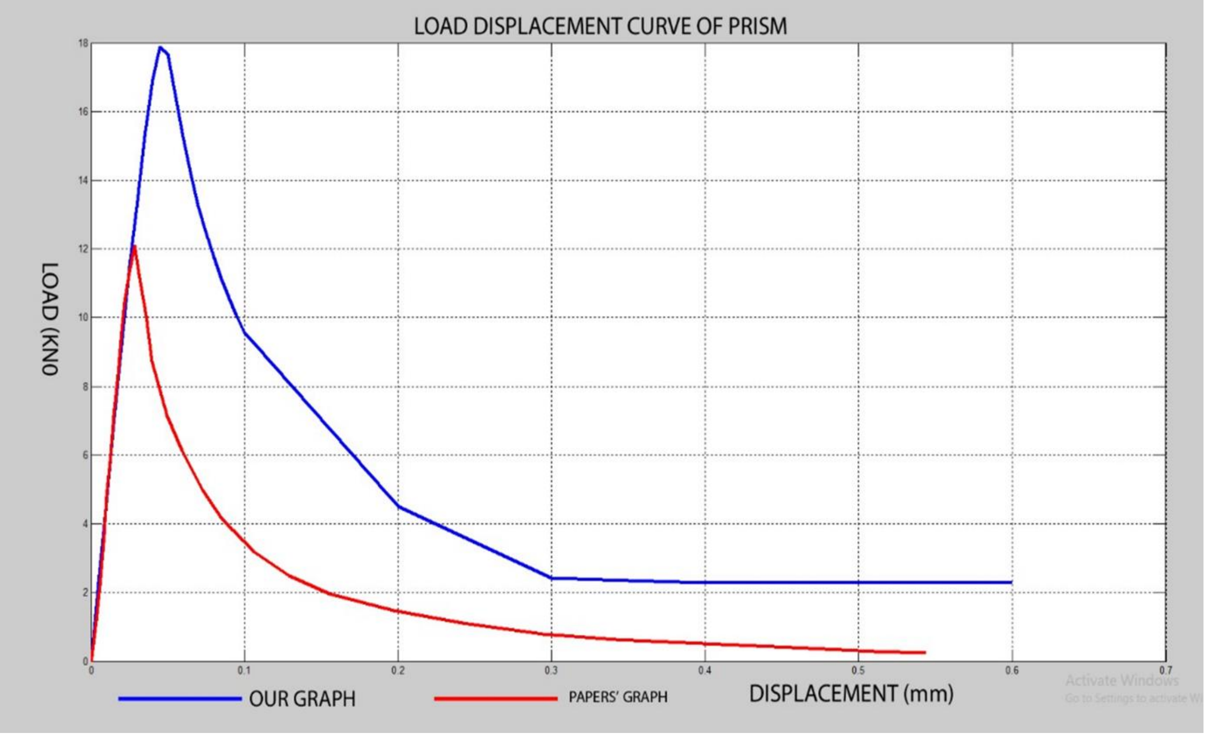

Figure 4. 1 (Result of load displacement curve of prism)

The graph in the blue shows the results of our model and the graph in the blue shows the experimental results were extracted from (Hamad et al., 2013) . The failure load calculated for the prism is 12KN as shown by the experimental results. It is the load corresponding to the maximum tension stress i.e. 10% of compression stress of the beam. However, our beam model fails at the 18KN. The difference is in the fictitious crack region of the beam.

As the elongation is increased, the curve should start to decline for the load, but the curve started increasing up to 18KN and then follows the declining branch. The difference in the model and experimental data is due to error in the code and could be resolved by eliminating the error from the code

4.2 Results for the Single crack in the beam:

The moment curvature is used to analyze the model of the single crack in the beam. Following are the results obtained:

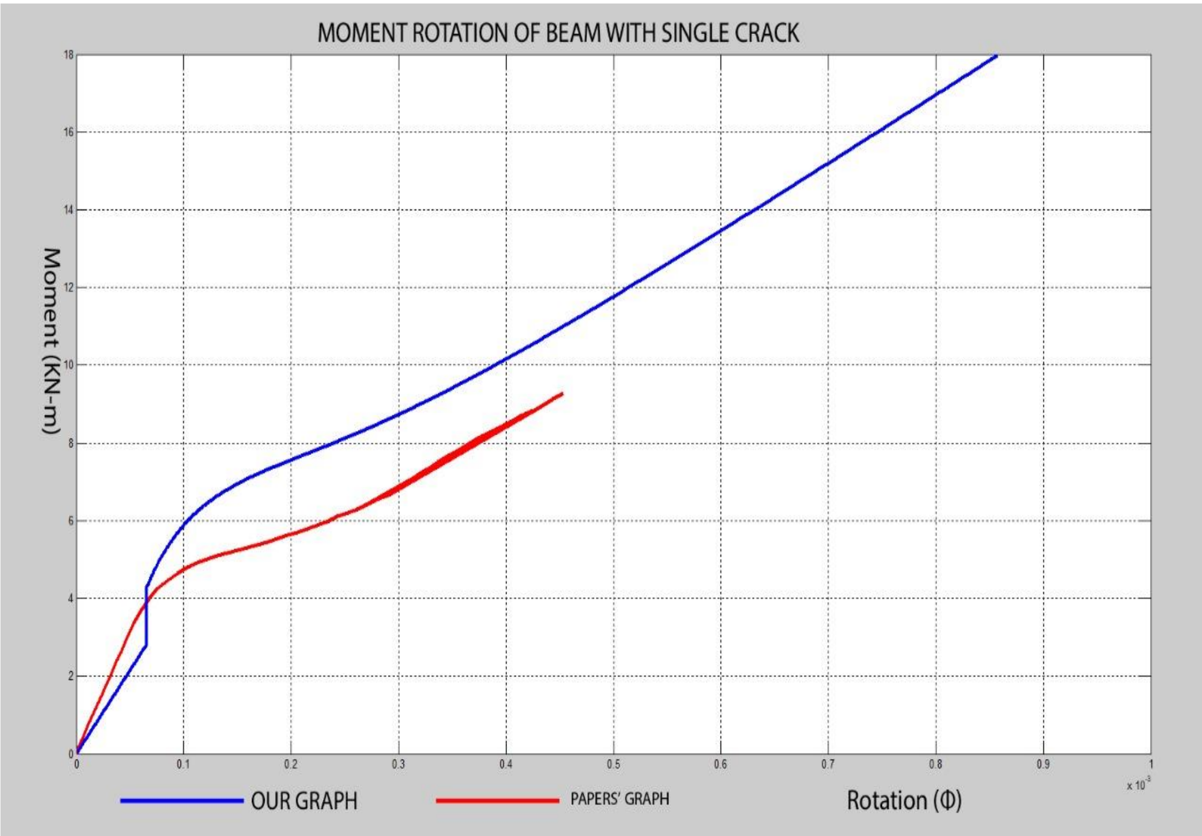

Figure 4. 2 (Result of moment rotation of model of beam with single crack)

From this result we can see that the model is almost replicated as compared to (Hamad et al., 2015) . The error in the previous result of the prism is rectified in this model as the fictitious crack zone has less effect in the reinforced beam. Therefore, the defect in the previous model is not incorporated in the model of single crack in the beam. The complete moment rotation curve is also developed for the beam.

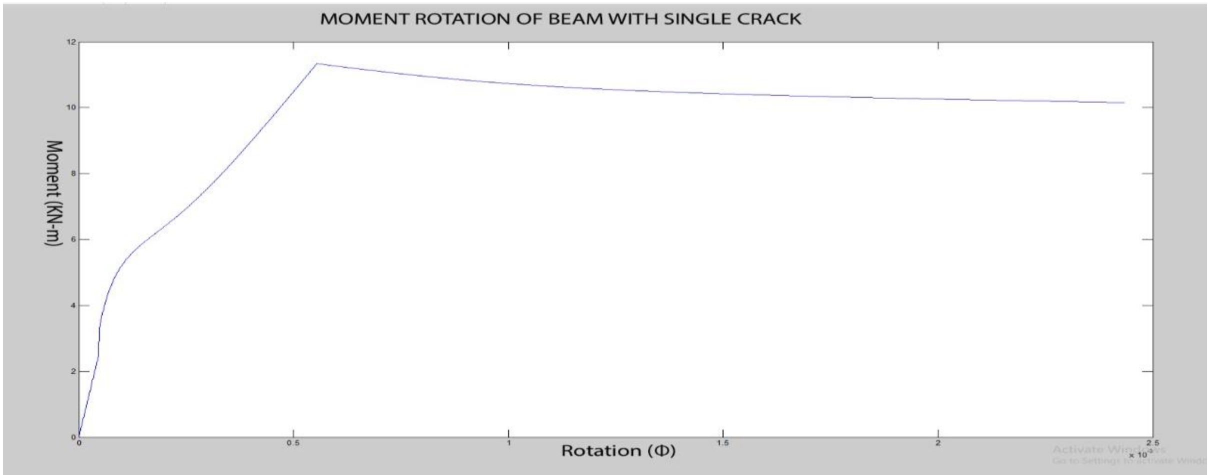

Figure 4. 3 (Result of moment rotation of whole beam with single crack)

This moment rotation curve also shows the trend followed by the beam and shows the failure moment of the beam which is 11.5KN-m. Now from the model it is also possible to obtain the results for the load deflection.

4.3 Results of Dynamic Analysis:

For the dynamic analysis, the response is used to estimate the resonant frequency at different damage levels but the results were not satisfactory. From the previous research of Hamad owen paper of 2011(Hamad et al., 2011), the single crack model of the beam should have the decreased resonant frequency of about 4.5% for the 80% damage on the beam but in our model, the frequency was 36.6Hz and doesn't change along the increasing damage in the beam. Following is the response for the undamaged state.

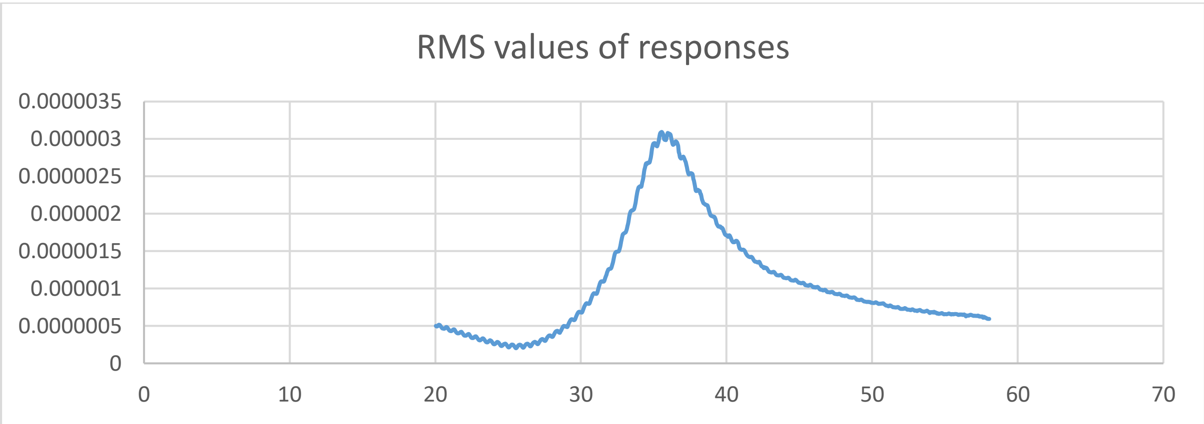

Figure 4. 4 (Result of RMS value of responses)

Therefore, more research needs to be carried out to correct the MATLAB code for the dynamic analysis as the results did not much satisfy any experimental or research-based data.

CHAPTER 5

CONCLUSIONS

The model of a crack in concrete is developed by ensuring the compatibility. This is done using the Newton-Raphson iterative solver. To calculate the moment and rotation in the cross-section, the Multi-Line method is used.

To calculate the stress from elongation profile, the compression region is solved using the Carriera and Chu equation. The tension region stresses are solved using the Fictitious crack theory model and steel is added at the cover of 37.5mm from the bottom.

Multi-Line Method:

This method is mainly used to calculate a moment corresponding to the certain rotation. First, a neutral axis is assumed and using the rotation and neutral axis, the elongation at the bottom fiber is calculated. From rotation and elongation of bottom fiber, the elongation profile is established by dividing the cross-section into smaller strips. From that elongation profile, the stress profile is established by calculating the stress at each strip from the equation according to compression and tension state of the strip. Then, the Forces in the cross-section are summed up. If it approaches to zero then the moment is calculated for each strip and then summed up, otherwise if the forces do not become zero, the neutral axis is changed and the whole process is repeated until forces becomes zero.

Newton-Raphson iterative solver:

To types of equations are proposed. One is G1 and other is G2. Both should be equal to zero to ensure the compatibility. To find the values of moment and rotation that gives G1 and G2 zero, Newton-Raphson iterative solver is used. At first, moment and rotation values are assumed zero and from the iterative process, the values of moment and rotation are calculated until the G1 and G2 becomes zero. In this way using the both Multi-line method and Newton-Raphson iterative solver, the moment and rotation values are calculated for a certain displacement.

Dynamic Analysis:

For the dynamic analysis, we need stiffness, damping and mass matrix. The beam is divided into 3 parts. Two parts are uncracked, and the middle part is cracked.

Stiffness:

The stiffness of uncracked region is taken as simple matrix and that of the cracked region is calculated by including the flexural rigidity in the stiffness matrix and then the global stiffness matrix is calculated.

Mass Matrix:

Consistent mass matrix is used instead of lumped mass matrix as it gives more accurate results.

Damping matrix:

Damping matrix is calculated using the Releigh damping. The frequencies used to calculate the constants are the 1st and 2nd undamped natural frequencies of the system in radian per second.

Sine sweep analysis:

Sine sweep wave is applied at a distance of 1.027m from the left support and the response of the beam is also analyzed at the same place. Time-stepped approach is used to apply the sine sweep. The time step of 0.04Hz is used and the frequency range used is 31-58Hz. The response vector is converted into the RMS value for each frequency and plotted. From the plot, the resonance frequency is calculated.

On the light of above following conclusion were made:

1. Single proliferation of cracks was projected successfully.
2. Flexure crack has been studied only, and shear cracks have been ignored.
3. With considerable results un notched crack is modelled.
4. The model shows in the dynamic simulation that the resonant frequency is weakly diminished with growing damage, and that much of this reduction happens just at early stages of damage.
5. The proposed model is used successfully in tackling the problem of reverse engineering, i.e. identifying a structure's damage state by vibration measurements.

RECOMMENDATIONS

Some recommendations proposed by us are as follows:

1. Due to covid-19 pandemic we were not able to cater for the shear effect in the computational modeling of concrete beams so future researchers should cater for the shear effect as well.

2. Since the modified stiffness matrix does not really compensate for shear effects, a method must be established which will also accommodate for the shear effect and more accurately model the crack.

CONSTRAINTS

However, although the predictions of the model are quantitatively comparable with the experimental results, the model has some limitations which restrict its application:

1. Due to the corona pandemic we were not able to perform experiments on the beams we have casted and therefore took the results from research (Hamad et al., 2013, 2015) but our results were having some errors due to some error in the code due to unknown reasons. But results were approximately correct.

2. The derivation of the updated matrix of stiffness (cracked regions) only acknowledges bending actions and neglects the shear consequences.

3. The model adopts simplified damping model in cracked RC beams to simulate the damping behavior.

4. In fact, the model adopts solid steel reinforcement bond-slip action at the undamaged sections and neglects bond-slip behavior at the broken areas.

REFERENCES

Anderson, T. L. (2017). Fracture Mechanics: Fundamentals and Applications, Fourth Edition. In *CRC Press*.

Bažant, Z. P. (2004). Scaling theory for quasibrittle structural failure. *Proceedings of the National Academy of Sciences of the United States of America*, *101*(37), 13400–13407. https://doi.org/10.1073/pnas.0404096101

Bažant, Z. P., & Oh, B. H. (1983). Crack band theory for fracture of concrete. *Matériaux et Constructions*. https://doi.org/10.1007/BF02486267

Bazant, Z. P., & Planas., J. (1998). Fracture and size effect in concrete and other quasibrittle structures. In *CRC press*.

Clough, R. W., & Penzien, J. (2010). Dynamic of Structures. In *Computer Methods in Applied Mechanics and Engineering*. https://doi.org/10.1088/1751-8113/44/8/085201

Hamad, W. I., Owen, J. S., & Hussein, M. F. M. (2011). The use of fictitious crack model in modelling the vibration behaviour of cracked reinforced concrete beams. *Proceedings of the 8th International Conference on Structural Dynamics, EURODYN 2011*, *September*, 2290–2297.

Hamad, W. I., Owen, J. S., & Hussein, M. F. M. (2013). An efficient approach of modelling the flexural cracking behaviour of un-notched plain concrete prisms subject to monotonic and cyclic loading. *Engineering Structures*, *51*, 36–50. https://doi.org/10.1016/j.engstruct.2013.01.007

Hamad, W. I., Owen, J. S., & Hussein, M. F. M. (2015). Modelling the degradation of vibration characteristics of reinforced concrete beams due to flexural damage. *Structural Control and Health Monitoring*. https://doi.org/10.1002/stc.1726

Hillerborg, A., Modéer, M., & Petersson, P. E. (1976). Analysis of crack formation and crack growth in concrete by means of fracture mechanics and finite elements. *Cement and Concrete Research*, *6*(6), 773–781. https://doi.org/10.1016/0008-8846(76)90007-7

Hordijk, D. A. (1992). Tensile and tensile fatigue behaviour of concrete; experiments, modelling and analyses. In *Heron* (Vol. 37, Issue 1, pp. 1–79).

Phillips, D. V., & Binsheng, Z. (1993). Direct tension tests on notched and un-notched plain concrete specimens. *Magazine of Concrete Research*. https://doi.org/10.1680/macr.1993.45.162.25

Reinhardt, H. W. (1984). FRACTURE MECHANICS OF AN ELASTIC SOFTENING MATERIAL LIKE CONCRETE. *Heron*.

Reinhardt, Hans W., Cornelissen, H. A., & Hordijk, D. A. (1986). Tensile tests and failure analysis of concrete. *Journal of Structural Engineering (United States)*. https://doi.org/10.1061/(ASCE)0733-9445(1986)112:11(2462)

Roesler, J., Paulino, G. H., Park, K., & Gaedicke, C. (2007). Concrete fracture prediction using bilinear softening. *Cement and Concrete Composites*. https://doi.org/10.1016/j.cemconcomp.2006.12.002

Rytter, A. (1993). Vibrational Based Inspection of Civil Engineering Structures. In *Fracture and Dynamics*. https://doi.org/10.1016/j.jsv.2016.06.047

Sancho, J. M., Planas, J., Cendón, D. A., Reyes, E., & Gálvez, J. C. (2007). An embedded crack model for finite element analysis of concrete fracture. *Engineering Fracture Mechanics*. https://doi.org/10.1016/j.engfracmech.2006.01.015

Sima, J. F., Roca, P., & Molins, C. (2008). Cyclic constitutive model for concrete. *Engineering Structures*. https://doi.org/10.1016/j.engstruct.2007.05.005

Sundara Raja Iyengar, K. T., Raviraj, S., & Jayaram, T. N. (2002). Analysis of crack propagation in strain-softening beams. *Engineering Fracture Mechanics*. https://doi.org/10.1016/S0013-7944(01)00093-5

Ulfkjrer, J. P., Krenk, S., & Brincker, R. (1995). Analytical model for fictitious crack propagation in concrete beams. *Journal of Engineering Mechanics*. https://doi.org/10.1061/(ASCE)0733-9399(1995)121:1(7)

APPENDIX

Code for the Newton-Raphson iterative solver:

```
clc
clear all
close all
Loop =1;
number = 1;   %Count for display
fprintf(' Table of Extension Stress, and Loads\n\n');
fprintf(' Number  Extension      Width       Stress    Compression Tension
Moment\n');
fprintf('              mm           mm          N/mm^2          N           N
Nmm\n');
fprintf(' ====== ===========    ======      ======    =========== ========
========\n');
%Defining variables%
w=0;
E = 41200;                    %E value in N/mm2
fcu = 30;                   %Compressive strength from the experiment N/mm2
div = 100;                      %No. of divisions
b=130;                        %mm
h=210;                        %mm
hc = b/2;
fct = fcu/10;
vct = (fct)*hc/E;
vx =0.0001;
%Initial Value of vx

%%%%%%%%%%%%%%%%%%%%%%%%%Forelastic range%%%%%%%%%%%%%%%%%%%%%%%%%%%%%%%%

%Stress = E * Strain
while vx <= vct

%%%%%%%%%%%%%%%%%%%%For Calculation of steel%%%%%%%%%%%%%%%%%
Steel_Sigma = 200000*(vx/hc);      %Reinforced concrete is introduced here
foreastic region
if Steel_Sigma > 250.460
Steel_Sigma = 250.460;
end
Steel_Forces = Steel_Sigma *258;

%%%%%%%%%%%%%%%%%%%%%%%%Steel%%%%%%%%%%%%%%%%%%%%%%%%%%%%%%%%%%%%%%%%%%%%%%

VTension = vx;
SigmaT = (E * VTension)/hc;

%Finding neutral axis%

f = @(y1) 1/2*b*y1*SigmaT-1/2*b*(h-y1)*((h-y1)/y1)*SigmaT + Steel_Forces;
y1 = fzero(f, [40,210]);                %Neutral axis from bottom
y2 = h-y1;                              %Neutral axis from top

%%%%%%%%%%%%%%%%%%%%%%%%%%%%Display Window%%%%%%%%%%%%%%%%%%%%%%%%%%%%

Pcomp = 1/2*b*(h-y1)*((h-y1)/y1)*SigmaT;
Ptension = 1/2*b*y1*SigmaT + Steel_Forces;
stress = E * vx/hc;
moment = ((y1*2/3)+50)*Ptension - (y2*1/3)*Pcomp +  Steel_Forces*(h-37.5);
```

```
%Tension Positive

out = [number,vx,w,stress,Pcomp,Ptension,moment];
fprintf (' %4d %11.4f %11.4f %11.4f %11.4f %11.4f %13.4f\n',out);
number = number + 1;

%%%%%%%%%%%%%%%%%%%%%%%%%%Display Window%%%%%%%%%%%%%%%%%%%%%%%%%%%

Moment(Loop) = moment;
phi(Loop) = atan(vx/y1);
Loop = Loop + 1;

vx = vx+0.0001;
end
Elastic_moment = moment;

%%%%%%%%%%%%%%%%%For inelastic region%%%%%%%%%%%%%%%%%%%%%%%%%%%%%%%%%%%%%
%Finding na%

C1 = 3;
C2 = 6.93;
Gf =  (43.3+1.13*fcu)/1000;    %Gf in N/m and fcu in MPa
wc = 5.14*(Gf/3.127);      %wc in mm
p3 = ((1+C1^3)*exp(-C2)) / wc;
p2 = -C2/wc;
p1 = (C1/wc)^3;
while vx>vct

%%%%%%%%%%%%%%%%%%%%%For Calculation of steel%%%%%%%%%%%%%%%%%

Steel_Sigma = 200000*(vx/hc);      %Reinforced concrete is introduced here
foreastic region
if Steel_Sigma > 250.46
Steel_Sigma = 250.460;
end
Steel_Forces = Steel_Sigma *258;

%%%%%%%%%%%%%%%%%%%%%%%%Steel%%%%%%%%%%%%%%%%%%%%%%%%%%%%%%%%%%%%%%%%%%

vdiff = vx-vct;
incre = vdiff/100;

%%%%% For Fictitious Curve %%%%%%%%%%%%

vparabolic = vct:incre:vx;
y=1;
for i=vparabolic
w = i-vct;
Stress(y)  =  fct*((1+(C1*(w/wc))^3)*exp(-C2*(w/wc))-(w/wc)*(1+C1^3)*exp(-
C2));
y=y+1;
 end
```

```
%%%%%%%%%%% For Compression curve %%%%%%%%%%%%%%%%%%%%%%%%%

%Chu equation for the compression area%
e0 = (7.1*fcu + 1680)*10.^-6;
Beta = 1/(1-(fcu/(E*e0)));
A = (fcu *Beta) / (hc*e0);
B = Beta - 1;
C = (1/(hc*e0));
fc =@(a) (A*a)./(B+(C*a).^Beta);     %CHU Equation
%It is the height of the sample from bottom throught which parabola will
occur = y1-((vct/vx)*y1)%
z = @(y1) sum(stress)*((y1-((vct/vx)*y1))/100)*b...
+ (fct*((vct/vx)*y1)*b*1/2) + Steel_Forces...
- sum(fc(0:((vx * (h-y1))/(y1*100)):(vx * (h-y1)/y1))) * b * (h-y1)/100;
y1 = fzero(z, [40 210]);
y2 = h-y1;



%%%%%%%%%% Moment in compression %%%%%%%%%%%%%%%%%%%

Strip_Length = (h-y1):-(h-y1)/100:0;
icre = 1;
Moment_Comp = 0;
for a = 0:((vx * (h-y1))/(y1*100)):(vx * (h-y1)/y1)
m = fc(a);
Moment_Comp = Moment_Comp + (m *b * (h-y1)/100*(Strip_Length(icre)));
icre =icre+1;
end

curvelength = y1-(vct/vx)*y1;
increment = curvelength/100;
moment_increment = 0:increment:curvelength;
moment = 0;
y=1;
for a=(stress)
moment = moment + a*b*increment*((h-(y1(vct/vx)*y1))+moment_increment(y));
y=y+1;
end
mom  =  +moment  +  (fct*((vct/vx)*y1)*b*1/2)*  (y2+((vct/vx)*y1)*(2/3))  -
Moment_Comp + Steel_Forces*(h-37.5);

%%%%%%%%%%%%%%%%%%%%Display Window%%%%%%%%%%%%%%%%%%%%%%%%%%%%%%%%%%%

Pcomp = ((h-y1)*1/2*b*(((h-y1)/y1))*(vx/hc)*E);
Ptension             =              sum(stress)*((y1-((vct/vx)*y1))/100)*b
+(fct*((vct/vx)*y1)*b*1/2);
stress1   =   fct*((1+(C1*(w/wc))^3)*exp(-C2*(w/wc))-(w/wc)*(1+C1^3)*exp(-
C2));
out = [number,vx,w,stress1,Pcomp,Ptension,mom];
fprintf (' %4d %11.4f %11.4f %11.4f %11.4f %11.4f %13.4f\n',out);
number = number+1;
Moment(Loop) = mom;
phi(Loop) = atan(vx/y1);
Loop = Loop + 1;
vx = vx+0.0001;
end
```

Code for Compatibility Ensurance using Jacobin:

```
clc
clear all
%Starting values
M = 0;
Theta1  = 0;
Del = [0:0.005:0.1 0.2:0.1:0.6];
a =1;
%Compatibility equations
for Delta = Del;
%Inputs
E = 41200;
I = (50*100.^3) / 12;
L1 = 100;
L2 = 25;
ws = 0.000002400 * 100 * 50;
hc =50;
%Starting values

M = 0;
Theta1  = 0;
ABC =1;
while ABC == 1
%G1 function
A = M - (ws*((L1+L2).^2/2));
B = ((L1+L2).^3 / 3) - (L1.^3/8) - (L1.^2*L2/6);
G1 = Theta1 + (A/(3*E*I))*L1 + (A/(E*I))*L2 + (ws/(E*I))*B - Delta/L1;
%G2 Function
if M == 0 && Theta1 ==0
kcr = (2*E*I)/hc;
else
phi = Theta1 * 2;
MomentFile = importdata('CheckM.mat');
PhiFile = importdata('CheckP.mat');
[val,idx]=min(abs(PhiFile-phi));
Mc = MomentFile(idx);
kcr = Mc/Theta1;
end
G2 = M - kcr*Theta1;

% Jacobin Solver

if M == 0 && (Theta1 == 0);
J = [1 L1/(3*E*I);0 1];
else
J = [1 L1/(3*E*I);(M-Mp)/(Theta1-Theta1p) 1];
end
X = [Theta1;M] - inv(J)*[G1;G2];
Mp = M;
Theta1p = Theta1;
Theta1 = X(1);
M = X(2);
if abs(M-Mp) < 30 && (abs(Theta1-Theta1p) < 0.000001) && (abs(G1) < 1) &&
(abs(G2) < 50)
Displacement(a) = Delta;
Force(a) = M/50000;
disp(Delta)
disp(M/50000)
a = a+1;
```

```
break
end
end
end
plot(Displacement,Force)
```

Note: In this code, the check M and check P are the Moment and rotation values extracted from the Newton-Raphson iterative solver.

Code for the dynamic analysis:

- **Stiffness matrix for uncracked region**

```
function [k]=beam_local_K(E,I,L);

k = (E)*[(12*I)/(L.^3) 6*I/L^2 -12*I/L^3 6*I/L^2;
    6*I/L^2 4*I/L -6*I/L^2 2*I/L;
    -12*I/L^3 -6*I/L^2 12*I/L^3 -6*I/L^2;
    6*I/L^2 2*I/L -6*I/L^2 4*I/L];
End
```

- **Stiffness for the cracked region**

```
function [k]=beam_local_KCracked(E,I,L);

 k = (E)*[(12*I)/(L.^3) 6*I/L^2 -12*I/L^3 6*I/L^2;
    6*I/L^2 3*I/L -6*I/L^2 3*I/L;
    -12*I/L^3 -6*I/L^2 12*I/L^3 -6*I/L^2;
    6*I/L^2 3*I/L -6*I/L^2 3*I/L];
End
```

- **Mass Matrix:**

```
function [m]=beam_local_M(b,h,l)

m = (0.0000024*b*h*l)*[156 22*l 54 -13*l;
    22*l 4*l.^2 13*l -3*l.^2;
    54 13*l 156 -22*l;
    -13*l -3*l.^2 -22*l 4*l.^2];
End
```

- **Code for calculating Global Matrices**

```
function [MG,KG,C] = Model(vx)
clear KG C MG
E_s = 199200;
E = 41200;
n = E_s / E;
b = 130;
h = 210;
hc = h/2;
A_s =   10*10/4*pi;         %Area of steel
I = b*205.32^3/12 + (n-1)*A_s;
%Total length of beam is considered 2700mm
```

```
L1 = 1297.5;%Total length of uncracked region in mm
L2 = 105;

%%%%%%%%%%%%%%%%%%%%%%%%%%%%%%%%%Mass Matrix%%%%%%%%%%%%%%%%%%%%%%%%%%%%

M1 = beam_local_M(b,h,L1);
M2 = beam_local_M(b,h,L2);
MG = zeros(8,8);

MG(1:4,1:4) = MG(1:4,1:4) + M1;
MG(3:6,3:6) = MG(3:6,3:6) + M2;
MG(5:8,5:8) = MG(5:8,5:8) + M1;

%%%%%%%%%%%%%%%%a0 and a1 Calculations%%%%%%%%%%%%%%%%%%%%%%%%%%%%

wm = 302.87;
wn = 1211.47;
zi = 0.05;

a0 = ((2*zi)/(wm+wn)) * (wm*wn);
a1 = ((2*zi)/(wm+wn)) * 1;

%%%%%%%%%%%%%%%%%Stiffness Matrix%%%%%%%%%%%%%%%%%%%%%%%%%%%%%%%%

K1 = beam_local_K(E,I,L1);          %K for uncracked region
K2 = beam_local_KCracked(E,I,L2);          %K for cracked region
KG = zeros(8,8);

KG(1:4,1:4) = KG(1:4,1:4) + K1;
KG(3:6,3:6) = KG(3:6,3:6) + K2;
KG(5:8,5:8) = KG(5:8,5:8) + K1;

for i = vx

if i == 0
alpha = (2*E*I)/hc;
else
clear I
[alpha,I] = kcr(i);
K1 = beam_local_K(E,I,L1);          %K for uncracked region
K2 = beam_local_KCracked(E,I,L2);          %K for cracked region
end
aprime = alpha/2;
KG(4,4) = KG(4,4) + aprime;
KG(6,6) = KG(6,6) + aprime;
KG(4,6) = KG(4,6) - aprime;
KG(6,4) = KG(6,4) - aprime;

%%%%%%%%%%%%%%%%%%%%%Damping Matrix%%%%%%%%%%%%%%%%%%%%%%%%%%

C = a0*MG + a1*KG;
clc
end
```

- **Main Code for Dynamic Analysis:**

```
clc
clear all
close all
vx =0.149;
j = 1;
for Elon = vx
[M,K,C] = Model(Elon);
f = 31;
a = 57;
A = [];
i = 1;
y0 = [[0;0;0;0;0;0;0;0] [0;0;0;0;0;0;0;0]];
while f<a
f = f + 0.1;
[x,y] = ode23t(@(t,y)equation(t,y,f,M,K,C),[0 2],y0);
y0 = y(size(y,1),:);
z = y(:,11);
A = [A;z];
result = 0;
Y(i) = mean(sqrt(z.^2));
X(i) = f;
i = i+1;
end
[val, idx] = max(Y, [], 2);
Frequency(j) = X(idx);
if Elon == 0
X1 = X;
Y1 = Y;
else
X2 = X;
Y2 = Y;
end
clear X Y
j=j+1;
end
```

- **Code for the equation of dynamic analysis:**

```
function dy = equation(t,y,f,M,K,C)

Ft = [0;0;sin(2*pi*f*t);0;0;0;0;0];
a =(-K) / M;
b = (-C) / M;
c = inv(M)*Ft;
zero = zeros(8,8);
I = [1 0 0 0 0 0 0 0;
     0 1 0 0 0 0 0 0;
     0 0 1 0 0 0 0 0;
     0 0 0 1 0 0 0 0;
     0 0 0 0 1 0 0 0;
     0 0 0 0 0 1 0 0;
     0 0 0 0 0 0 1 0;
     0 0 0 0 0 0 0 1];

dy=([zeroI;ab]*[y(1);y(2);y(3);y(4);y(5);y(6);y(7);y(8);y(9);y(10);y(11);
y(12);y(13);y(14);y(15);y(16)]) + [0;0;0;0;0;0;0;0;c];
end;
```